

## Title page

# Can dual energy CT with fast kV-switching determine renal stone composition accurately?

Bo Mussmann<sup>1,2,3</sup>, Maryann Hardy<sup>2,4</sup>, Helene Jung<sup>5</sup>, Ming Ding<sup>6,7</sup>, Palle J. Oster<sup>5</sup>, Ole Graumann<sup>1,2</sup>

1. Department of Radiology, Odense University Hospital, Denmark
2. Research and Innovation Unit of Radiology, University of Southern Denmark
3. Faculty of Health Sciences, Oslo Metropolitan University, Norway
4. Faculty of Health Studies, University of Bradford, UK
5. Urological Research Center, Department of Urology, Lillebaelt Hospital, Vejle, Denmark
6. Department of Orthopaedic surgery and traumatology, Odense University Hospital, DK
7. Department of Clinical Research, University of Southern Denmark

Corresponding author:

Bo Mussmann

Department of Radiology, Odense University Hospital, Denmark

Sdr. Boulevard 29

5000 Odense C, Denmark

e-mail: [bo.mussmann@rsyd.dk](mailto:bo.mussmann@rsyd.dk)

Declarations of interest: none

1 **Can dual energy CT with fast kV-switching determine renal stone composition accurately?**  
2  
3

4 **Abstract**  
5  
6  
7

8 **Rationale and objectives**  
9

10 To determine whether a single source CT system utilizing fast kV switching and low dose settings  
11 can characterize (diameter and chemical composition) renal stones accurately when compared  
12 infrared spectroscopy  
13  
14  
15  
16  
17  
18  
19

20 **Materials and methods**  
21

22 The chemical composition of 15 renal stones was determined using Fourier transform infrared  
23 spectroscopy. The stones were inserted into a porcine kidney and placed within a water tank for CT  
24 scanning using both fast kV switching dual energy and standard protocols. Effective atomic number  
25 of each stone was measured using scanner software. Stone diameter measurements were repeated  
26 twice to determine intra-rater variation and compared to actual stone diameter as measured by micro  
27 CT.  
28  
29  
30  
31  
32  
33  
34  
35  
36  
37  
38

39 **Results**  
40

41 The chemical composition of three stones (1 calcium phosphate and 2 carbonite apatite) could not  
42 be determined using the scanner software. The composition of 10/12 remaining stones was correctly  
43 identified using DECT (83% absolute agreement;  $k=0.69$ ). No statistical difference ( $p=0.051$ ) was  
44 noted in the mean stone diameter as measured by clinical CT and micro CT.  
45  
46  
47  
48  
49  
50  
51  
52

53 **Conclusion**  
54

55 DECT using fast kV switching may potentially be developed as a low dose clinical tool for  
56 identifying and classifying renal stones in vivo supporting clinical decision-making.  
57  
58  
59  
60  
61  
62  
63  
64  
65

1  
2  
3  
4  
5  
6  
7  
8  
9  
10  
11  
12  
13  
14  
15  
16  
17  
18  
19  
20  
21  
22  
23  
24  
25  
26  
27  
28  
29  
30  
31  
32  
33  
34  
35  
36  
37  
38  
39  
40  
41  
42  
43  
44  
45  
46  
47  
48  
49  
50  
51  
52  
53  
54  
55  
56  
57  
58  
59  
60  
61  
62  
63  
64  
65

**Keywords**

Renal Stone; urolithiasis; dual energy computed tomography; micro CT

1 **Introduction**  
2  
3

4 Non-contrast computed tomography is the first-line imaging modality for patients with acute flank  
5 pain (1-3). However, the associated radiation risk remains a concern, particularly as the incidence of  
6 renal stones has increased over the recent years due to increasing levels of obesity and lifestyle  
7 changes both among children and adults (4-6). The chemical components of renal stones vary  
8 depending on the underlying causal agent. Calcium Oxalate (CaOx) stones are the most commonly  
9 occurring stone types accounting for 70% of cases while calcium phosphate, uric acid and cystine  
10 account for about 20%, 8% and 2% of cases respectively (7). Other stone types such as struvite  
11 occur more rarely; however, it is crucial that the chemical composition of the stone is accurately  
12 determined as this will guide the clinician in treatment planning (e.g. shock wave lithotripsy  
13 (SWL); endoscopic stone removal; lifestyle changes; pharmacological intervention) (7, 8). Spectral  
14 analysis of renal stones for analyzing chemical composition is advocated within clinical guidelines,  
15 (9) but can only be performed where the stone has been surgically removed or collected after  
16 spontaneous passage. Reliable in vivo stone analysis could have major importance for choice of  
17 treatment; i.e. if imaging clearly defines the stone as a cystine stone, this will direct the clinician to  
18 endoscopic methods for stone management, since cystine calculi are most often SWL resistant.  
19 Furthermore, such a finding would prone the clinician to perform an early metabolic evaluation, in  
20 order to start stone preventive therapy. Another example could be imaging clearly showing uric acid  
21 that often may be treated by oral litholysis, sparing patients for invasive treatments, and directing  
22 the clinician to look for metabolic syndrome (MS), since uric acid stone disease is often  
23 linked to MS that would need dietary advices for both stone prevention and other potential harmful  
24 effects of MS. In both these examples in vivo stone analysis potentially could change clinical  
25 management and lead to earlier preventive measures, thereby personalizing stone management up-  
26 front.  
27  
28  
29  
30  
31  
32  
33  
34  
35  
36  
37  
38  
39  
40  
41  
42  
43  
44  
45  
46  
47  
48  
49  
50  
51  
52  
53  
54  
55  
56  
57  
58  
59  
60  
61  
62  
63  
64  
65

1 For in vivo stone composition determination, the Hounsfield Units (HU) derived from standard  
2  
3 120kV single energy Computed Tomography (CT) have been proposed as an alternative approach  
4  
5 with good ability to differentiate uric acid from calcium stones (10), although accuracy of  
6  
7 classification is acknowledged to be influenced by stone size (11). The ability of single energy CT  
8  
9 to differentiate between the less common cystine and struvite stones is recognized to be limited due  
10  
11 to similarity and overlap in density and recorded HU values (12). In contrast, dual energy CT  
12  
13 (DECT) using two x-ray tubes has been shown to be reasonably effective in differentiating between  
14  
15 all stone types (13-21), but this technology is not routinely available within the general clinical  
16  
17 setting and therefore its application to clinical practice is limited. Only a small number of studies  
18  
19 have considered alternative approaches to achieving dual energy CT (e.g. sandwich detector; fast  
20  
21 kV switching) (7, 12, 22-25). Importantly, studies evaluating sandwich detector technologies found  
22  
23 low accuracy in chemical stone composition, especially at low dose (24, 25). In contrast while those  
24  
25 studies considering fast kV switching reported inconsistent findings in the accuracy of chemical  
26  
27 composition analysis, although it was noted that the CT technology used (40mm detector coverage)  
28  
29 did not reflect scanner quality currently available (80-160mm detector coverage). No study using  
30  
31 fast kV switching or sandwich detector technology as a method of dual energy CT imaging has  
32  
33 specifically considered low dose (effective dose <3mSv (26)) scanning options in the detection and  
34  
35 analysis of renal stones. Further, existing studies have focused their analysis on stones measuring  
36  
37 >5mm. This experimental study was undertaken to determine whether a single source CT system  
38  
39 (80-160mm detector coverage) utilizing fast kV switching, larger z-coverage and low dose settings  
40  
41 may characterize renal stones accurately when compared to infrared (IR) spectroscopy as the  
42  
43 laboratory reference standard.  
44  
45  
46  
47  
48  
49  
50  
51  
52  
53  
54  
55  
56  
57  
58

## 59 **Materials and methods**

60  
61  
62  
63  
64  
65

1 As this was an experimental study using a porcine kidney acquired from the meat industry, ethical  
2  
3 approval was waived in accordance with Danish legislation and approval for data acquisition  
4  
5 regarding stones was provided by the hospital manager (Journal no. 19/33519).  
6  
7

### 8 9 *Micro-CT analysis*

10  
11 Fifteen renal stones were percutaneously removed from 15 patients (8 female, 6 male, 1 unknown;  
12  
13 median age 53 years, age range 13 - 74 years) and chemical composition was determined using  
14  
15 Fourier transform infrared (IR) spectroscopy. The largest diameter of the stones was determined  
16  
17 using a Scanco  $\mu$ CT50 (5 stones) or Scanco VivaCT40 (10 stones) micro CT scanner (Scanco  
18  
19 Medical, Brüttisellen, Switzerland) with a tube voltage of 70 kV, tube current of 114  $\mu$ A, 0.5 mm  
20  
21 Al physical filter and 1200 mgHA beam hardening correction. The voxel size was 5 and 10.5  $\mu$ m in  
22  
23 the two scanners, respectively. Each stone was positioned in the bottom of a  $\varnothing$ 9mm tube and fixed  
24  
25 with foam to avoid movement during scanning. The stones were manually contoured on 2D images  
26  
27 and segmented using the scanner workstation and 3D renderings were generated and the maximum  
28  
29 diameter was measured (Fig. 1). The dimension of each stone was measured in the x, y and z planes  
30  
31 with the largest diameter considered representative of stone size.  
32  
33  
34  
35  
36  
37  
38  
39  
40  
41  
42

### 43 *Experimental setup*

44  
45  
46 The experiment replicated the approach taken by Talso et al (2018) (27). The stones were  
47  
48 individually inserted into a porcine kidney partly opened with a coronal cut (Fig. 2). The porcine  
49  
50 kidney was immersed in a 36 x 39 x 17cm water tank filled with 12 liters of tap water to mimic the  
51  
52 absorption of human tissue (Fig. 3) and scanned using a GE Revolution CT scanner (GE  
53  
54 Healthcare, Waukesha, IL, USA). Scans were acquired using both fast kV switching dual energy  
55  
56  
57  
58  
59  
60  
61  
62  
63  
64  
65

1 technique and standard helical protocol to permit comparison of radiation dose. Scan parameters are  
2  
3 listed in table 1.  
4  
5  
6  
7  
8  
9

### 10 *Image analysis*

11  
12  
13 The images were analyzed by a senior radiographer (BM) with >20 years of experience using a GE  
14 Advantage Workstation Volumeshare 7 (GE Healthcare, Waukesha, IL, USA). A circular 1.82 mm<sup>2</sup>  
15  
16 region of interest (ROI) was positioned in the center of each stone using the three orthogonal planes  
17  
18 to guide ROI positioning. Effective atomic number ( $Z_{\text{eff}}$ ) histograms were created for the ROIs and  
19  
20 the histograms were compared with the  $Z_{\text{eff}}$  of preprogrammed scanner library of different materials  
21  
22 (NIST curves, National Institute of Science and Technology) (Fig. 4). The observer was blinded to  
23  
24 the chemical composition of the stones as determined by IR spectroscopy. Maximum stone diameter  
25  
26 was measured using window-width of 300HU and window-level of 35HU and repeated after one  
27  
28 week to determine intra-rater variation. Mean attenuation and noise was measured in water and  
29  
30 kidney tissue using a 10 mm circular ROI. All image analyses were performed using 0.625 mm  
31  
32 slice thickness.  
33  
34  
35  
36  
37  
38  
39  
40

### 41 *Statistical analysis*

42  
43  
44 Continuous variables were summarized by descriptive statistics. Absolute agreement between IR  
45  
46 spectroscopy and DECT composition analysis was determined and Cohen's kappa calculated and  
47  
48 interpreted according to the thresholds outlined by Landis and Koch (28). Stone diameter, as  
49  
50 measured by clinical CT and micro CT, was tested for normality using the Shapiro-Wilk test and  
51  
52 differences were tested using paired t-test. A Bland-Altman plot was generated for assessment of  
53  
54 limits of agreement between repeated measurements. All analyses were performed using STATA/IC  
55  
56  
57  
58  
59 16.0 (StataCorp. LP, College Station, TX, USA).  
60  
61  
62  
63  
64  
65

1  
2  
3  
4  
5  
6  
7  
8  
9  
10  
11  
12  
13  
14  
15  
16  
17  
18  
19  
20  
21  
22  
23  
24  
25  
26  
27  
28  
29  
30  
31  
32  
33  
34  
35  
36  
37  
38  
39  
40  
41  
42  
43  
44  
45  
46  
47  
48  
49  
50  
51  
52  
53  
54  
55  
56  
57  
58  
59  
60  
61  
62  
63  
64  
65

## Results

While 15 stones were scanned and included in the analysis of stone diameter, 3 stones (1 calcium phosphate and 2 carbonite apatite) were excluded from the composition analysis due to the underlying composition data being absent from the CT scanner library of different materials.

### *Stone diameter and composition*

No statistical difference ( $p=0.051$ ) was noted in the mean stone diameter as measured by clinical CT (mean 4.0 mm; SD=1.18; range 2.2-5.1mm) and micro CT (mean 3.5mm; SD=1.6; range 0.88-6.22mm) or between first and second measurement in clinical CT (mean difference 0.04 mm,  $p=0.3$ ). The Bland-Altman limits of agreement for the repeated measurements also illustrated narrow variation in measures (-0.25 to 0.33 mm) (Fig. 5).

The composition of 10/12 stones was correctly identified using DECT (83% absolute agreement; Cohen's kappa 0.69). All cystine, uric acid and struvite stones were correctly identified. The brushite stone was characterized as CaOx and one CaOx stone was characterized as cystine (Table 2).

### *Radiation dose*

The mean Dose-Length Product (DLP) was 185.29 mGy\*cm (SD 3.94) in DECT versus 68.95 mGy\*cm (SD 3.41) in single energy mode. Using the conversion factor proposed by Dougeni et al (2012) (29) the measured DLP values translate into an estimated effective dose of 2.78 mSv and 1.03 mSv for dual and single energy mode respectively.



1  
2  
3  
4  
5  
6  
7  
8  
9  
10  
11  
12  
13  
14  
15  
16  
17  
18  
19  
20  
21  
22  
23  
24  
25  
26  
27  
28  
29  
30  
31  
32  
33  
34  
35  
36  
37  
38  
39  
40  
41  
42  
43  
44  
45  
46  
47  
48  
49  
50  
51  
52  
53  
54  
55  
56  
57  
58  
59  
60  
61  
62  
63  
64  
65

**Discussion**

In this experimental ex-vivo study using a porcine kidney, we found substantial agreement between infrared spectroscopy and DECT based characterization of renal stone type. The results are in line with previous studies performed using an older scanner model (12, 22). However, we have demonstrated that accurate stone classification can be achieved using a substantially lower radiation dose opening up the possibilities for wider clinical application for renal stone screening using CT technology. While the data from this study is not directly comparable to previous studies, our findings provide new insights into technological advances and opportunities for dose reduction.

Importantly, previous authors have reported CTDI<sub>vol</sub> estimates of 19.11 mGy (23) and 10.73 mGy (22) in DECT, estimates at least 34% greater than that achieved in current study (Table 1). Our study also adds clinical legitimacy to stone diameter measurements undertaken by clinical CT as it included stones ranging in diameter from 0.88-6.22mm (mean diameter 3.5mm), whereas previous studies had a wider range including larger stone diameters (mean diameters >5mm).

While agreement in chemical composition between IR spectroscopy and DECT was not perfect, the results suggest that stone composition may be determined using fast kV switching DECT. The erroneous results for the brushite stone was probably related to rounding of the numeric result to nearest chemical element as the effective Z of brushite is 14.1 versus 13.8 for CaOx (i.e. a difference <0.5) making the difference problematic to detect (30). In contrast, the cystine stone characterized as CaOx was particularly small (diameter of 3.2 x 3.1 x 1.7 mm as measured by micro CT) and we speculate that the erroneous classification may be a result of partial volume effect as the smallest diameter measurement was less than three pixels. However, other stones of similar sizes were correctly characterized and so further work is required to confirm this.

1  
2  
3  
4 *Limitations*  
5  
6

7 This study has a number of limitations. Firstly, the study included only a small sample of renal  
8 stones compared to previously published studies. However, these stones were generally small in  
9 diameter and better reflected current clinical investigative referrals, particularly where CT screening  
10 is in place. The composition of the stones in the sample was also not representative of a normal  
11 clinical sample, since a greater proportion of cystine stones was present. However, this does not  
12 invalidate the measurement data or the CT composition data presented above. The study did not  
13 differentiate between calcium monohydrate and calcium dihydrate which would be important from  
14 a clinical perspective, but at present it is not possible to distinguish between the two with the current  
15 technology. In an experimental study Duan et al (2013) (30) suggested analyzing the roughness of  
16 the stone surface using a shape index. The authors demonstrated reasonable accuracy, but  
17 apparently the method has not yet been tested clinically and it is not generally available. A further  
18 limitation was the use of a water tank of fixed size as this did not reflect the complexity of the  
19 abdomen or diversity of patient body habitus. Further studies investigating the clinical feasibility in  
20 vivo are needed and NIST curves for materials such as carbonite apatite must be incorporated into  
21 the scanner software and tested before implementation. In addition, it must be noted that while the  
22 dose in both single and dual energy CT was relatively low in this study, the DECT protocol, if  
23 adopted, would expose a patient to approximately 3 times the radiation dose (CTDIvol 7.15mGy)  
24 compared to standard single energy CT (CTDIvol 2.60mGy) and clinical assessment of its  
25 implementation should be undertaken. The dose difference in DECT is caused by a conservative  
26 protocol setup with restricted tube current modulation aiming to ensure data quality in the low kV  
27 dataset, and further investigation with regard to dose reduction is needed.  
28  
29  
30  
31  
32  
33  
34  
35  
36  
37  
38  
39  
40  
41  
42  
43  
44  
45  
46  
47  
48  
49  
50  
51  
52  
53  
54  
55  
56  
57  
58  
59  
60  
61  
62  
63  
64  
65

1 *Conclusion*

2  
3  
4 In conclusion, DECT with fast kV switching has very promising potentially as a clinical tool for  
5  
6 identifying and classifying renal stones. Further research is needed before DECT with fast kV  
7  
8 switching can be implemented as first line imaging tool in clinical practice.  
9  
10  
11  
12  
13  
14  
15  
16  
17  
18  
19  
20  
21  
22  
23  
24

25  
26 **References**

- 27  
28  
29 1. Jung H, Andonian S, Assimos D, Averch T, Geavlete P, Kohjimoto Y, et al. Urolithiasis: evaluation,  
30 dietary factors, and medical management: an update of the 2014 SIU-ICUD international  
31 consultation on stone disease. *World J Urol.* 2017;35(9):1331-40.  
32  
33  
34  
35 2. Lipkin M, Ackerman A. Imaging for urolithiasis: standards, trends, and radiation exposure. *Curr*  
36 *Opin Urol.* 2016;26(1):56-62.  
37  
38  
39  
40 3. Karmazyn B, Frush DP, Applegate KE, Maxfield C, Cohen MD, Jones RP. CT with a computer-  
41 simulated dose reduction technique for detection of pediatric nephroureterolithiasis: comparison  
42 of standard and reduced radiation doses. *Am J Roentgenol.* 2009;192(1):143-9.  
43  
44  
45 4. Bonzo JR, Tasian GE. The Emergence of Kidney Stone Disease During Childhood-Impact on Adults.  
46 *Curr Urol Rep.* 2017;18(6):44.  
47  
48  
49  
50 5. Ristau BT, Dudley AG, Casella DP, Dwyer ME, Fox JA, Cannon GM, et al. Tracking of radiation  
51 exposure in pediatric stone patients: The time is now. *J Pediatr Urol.* 2015;11(6):339.e1-5.  
52  
53  
54  
55  
56  
57  
58  
59  
60  
61  
62  
63  
64  
65

1  
2  
3  
4  
5  
6  
7  
8  
9  
10  
11  
12  
13  
14  
15  
16  
17  
18  
19  
20  
21  
22  
23  
24  
25  
26  
27  
28  
29  
30  
31  
32  
33  
34  
35  
36  
37  
38  
39  
40  
41  
42  
43  
44  
45  
46  
47  
48  
49  
50  
51  
52  
53  
54  
55  
56  
57  
58  
59  
60  
61  
62  
63  
64  
65

6. Clayton DB, Pope JC. The increasing pediatric stone disease problem. *Ther Adv Urol.* 2011;3(1):3-12.
7. Corbett J-H, Harmse WS. In vivo determination of renal stone composition with dual-energy computed tomography. *SA J Radiol.* 2014;18:1-5.
8. Andreassen KH, Pedersen KV, Osther SS, Jung HU, Lildal SK, Osther PJS. How should patients with cystine stone disease be evaluated and treated in the twenty-first century? *Urolithiasis.* 2016;44(1):65-76.
9. Turk C, Petrik A, Sarica K, Seitz C, Skolarikos A, Straub M, et al. EAU Guidelines on Diagnosis and Conservative Management of Urolithiasis. *Eur Urol.* 2016;69(3):468-74.
10. Primak AN, Fletcher JG, Vrtiska TJ, Dzyubak OP, Lieske JC, Jackson ME, et al. Noninvasive differentiation of uric acid versus non-uric acid kidney stones using dual-energy CT. *Acad Radiol.* 2007;14(12):1441-7.
11. Stewart G, Johnson L, Ganesh H, Davenport D, Smelser W, Crispin P, et al. Stone Size Limits the Use of Hounsfield Units for Prediction of Calcium Oxalate Stone Composition. *Urology.* 2015;85(2):292-5.
12. Joshi M, Langan DA, M.D. DSS, M.D. AK, Aluri S, Procknow K, et al. Effective atomic number accuracy for kidney stone characterization using spectral CT: SPIE; 2010.
13. Matlaga BR, Kawamoto S, Fishman E. Dual source computed tomography: a novel technique to determine stone composition. *Urology.* 2008;72(5):1164-8.
14. Stolzmann P, Leschka S, Scheffel H, Rentsch K, Baumuller S, Desbiolles L, et al. Characterization of urinary stones with dual-energy CT: improved differentiation using a tin filter. *Invest Radiol.* 2010;45(1):1-6.
15. Qu M, Ramirez-Giraldo JC, Leng S, Williams JC, Vrtiska TJ, Lieske JC, et al. Dual-energy dual-source CT with additional spectral filtration can improve the differentiation of non-uric acid renal stones: an ex vivo phantom study. *Am J Roentgenol.* 2011;196(6):1279-87.

- 1 16. Fung GS, Kawamoto S, Matlaga BR, Taguchi K, Zhou X, Fishman EK, et al. Differentiation of kidney  
2 stones using dual-energy CT with and without a tin filter. *Am J Roentgenol.* 2012;198(6):1380-6.  
3  
4  
5  
6 17. Acharya S, Goyal A, Bhalla AS, Sharma R, Seth A, Gupta AK. In vivo characterization of urinary  
7 calculi on dual-energy CT: going a step ahead with sub-differentiation of calcium stones. *Acta*  
8 *Radiol.* 2015;56(7):881-9.  
9  
10  
11  
12 18. Wilhelm K, Schoenthaler M, Hein S, Adams F, Schlager D, Kuehhas FE, et al. Focused Dual-energy  
13 CT Maintains Diagnostic and Compositional Accuracy for Urolithiasis Using Ultralow-dose  
14 Noncontrast CT. *Urology.* 2015;86(6):1097-102.  
15  
16  
17  
18  
19 19. Lombardo F, Bonatti M, Zamboni GA, Avesani G, Oberhofer N, Bonelli M, et al. Uric acid versus  
20 non-uric acid renal stones: in vivo differentiation with spectral CT. *Clin Radiol.* 2017;72(6):490-6.  
21  
22  
23  
24 20. Bonatti M, Lombardo F, Zamboni GA, Pernter P, Pycha A, Mucelli RP, et al. Renal stones  
25 composition in vivo determination: comparison between 100/Sn140 kV dual-energy CT and 120  
26 kV single-energy CT. *Urolithiasis.* 2017;45(3):255-61.  
27  
28  
29  
30  
31 21. Manglaviti G, Tresoldi S, Guerrer CS, Di Leo G, Montanari E, Sardanelli F, et al. In Vivo Evaluation  
32 of the Chemical Composition of Urinary Stones Using Dual-Energy CT. *Am J Roentgenol.*  
33 2011;197(1):W76-W83.  
34  
35  
36  
37  
38 22. Rompsaithong U, Jongjitaree K, Korpraphong P, Woranisarakul V, Taweemonkongsap T, Nualyong  
39 C, et al. Characterization of renal stone composition by using fast kilovoltage switching dual-  
40 energy computed tomography compared to laboratory stone analysis: a pilot study. *Abdominal*  
41 *radiology (New York).* 2019;44(3):1027-32.  
42  
43  
44  
45  
46  
47 23. Kulkarni NM, Eisner BH, Pinho DF, Joshi MC, Kambadakone AR, Sahani DV. Determination of Renal  
48 Stone Composition in Phantom and Patients Using Single-Source Dual-Energy Computed  
49 Tomography. *J Comput Assist Tomogr.* 2013;37(1):37-45.  
50  
51  
52  
53  
54  
55  
56  
57  
58  
59  
60  
61  
62  
63  
64  
65

- 1 24. Hidas G, Eliahou R, Duvdevani M, Coulon P, Lemaitre L, Gofrit ON, et al. Determination of Renal  
2 Stone Composition with Dual-Energy CT: In Vivo Analysis and Comparison with X-ray Diffraction.  
3 Radiology. 2010;257(2):394-401.  
4  
5  
6  
7  
8 25. Grosse Hokamp N, Salem J, Hesse A, Holz JA, Ritter M, Heidenreich A, et al. Low-Dose  
9 Characterization of Kidney Stones Using Spectral Detector Computed Tomography: An Ex Vivo  
10 Study. Invest Radiol. 2018;53(8):457-62.  
11  
12  
13  
14  
15 26. Drake T, Jain N, Bryant T, Wilson I, Somani BK. Should low-dose computed tomography kidneys,  
16 ureter and bladder be the new investigation of choice in suspected renal colic?: A systematic  
17 review. Indian J Urol. 2014;30(2):137-43.  
18  
19  
20  
21  
22 27. Talso M, Emiliani E, Froio S, Gallioli A, Forzenigo L, Pradere B, et al. Low-dose CT scan in stone  
23 detection for stone treatment follow-up: is there a relation between stone composition and  
24 radiation delivery? Study on a porcine-kidney model. Minerva Urol Nefrol. 2019;71(1):63-71.  
25  
26  
27  
28  
29 28. Landis JR, Koch GG. The Measurement of Observer Agreement for Categorical Data. Biometrics.  
30 1977;33(1):159-74.  
31  
32  
33  
34 29. Dougeni E, Faulkner K, Panayiotakis G. A review of patient dose and optimisation methods in adult  
35 and paediatric CT scanning. Eur J Radiol. 2012;81(4):e665-83.  
36  
37  
38  
39 30. Duan X, Qu M, Wang J, Trevathan J, Vrtiska T, Williams JC, Jr., et al. Differentiation of calcium  
40 oxalate monohydrate and calcium oxalate dihydrate stones using quantitative morphological  
41 information from micro-computerized and clinical computerized tomography. J Urol.  
42  
43  
44  
45  
46 2013;189(6):2350-6.  
47  
48  
49  
50  
51  
52  
53  
54  
55  
56  
57  
58  
59  
60  
61  
62  
63  
64  
65

1  
2  
3  
4  
5  
6  
7  
8  
9  
10  
11  
12  
13  
14  
15  
16  
17  
18  
19  
20  
21  
22  
23  
24  
25  
26  
27  
28  
29  
30  
31  
32  
33  
34  
35  
36  
37  
38  
39  
40  
41  
42  
43  
44  
45  
46  
47  
48  
49  
50  
51  
52  
53  
54  
55  
56  
57  
58  
59  
60  
61  
62  
63  
64  
65

**Figure and table legends**

**Fig. 1** Three-dimensional rendering (left) and a micro CT cross section of a Ø6.2 mm cystine stone (right)

**Fig. 2** Renal stone (arrow) positioned in the pelvis of a porcine kidney.

**Fig. 3** Porcine kidney immersed in a water tank with the kidney positioned in a smaller plastic container glued to the water tank to keep the kidney in place during the scan procedure.

**Fig.4.** ROI positioned in a cystine stone (left) and the corresponding histogram showing the effective atomic numbers in the ROI (right).

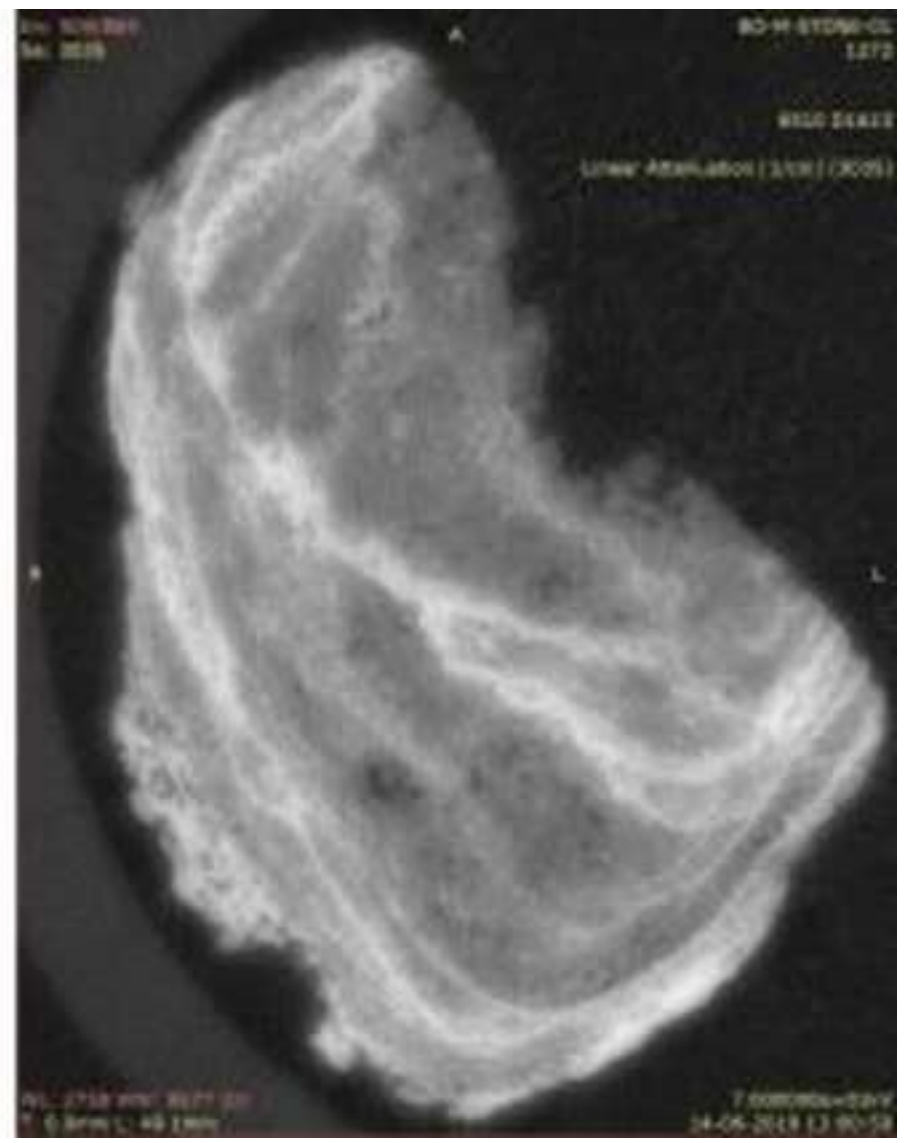
**Fig. 5** Bland-Altman plot of repeated stone diameter measurements. The upper and lower horizontal lines indicate limits of agreement and the middle line indicate mean difference between the measurements. N=15.

All figures should be reproduced in color

**Table 1** Scan parameters in standard helical and dual energy mode (\*Adaptive Statistical Iterative Reconstruction)

**Table 2** Agreement between IR spectroscopy and DECT composition analysis.

**Table 3** Mean attenuation (HU) and standard deviation (SD) in water and kidney tissue measured in standard helical and dual energy CT









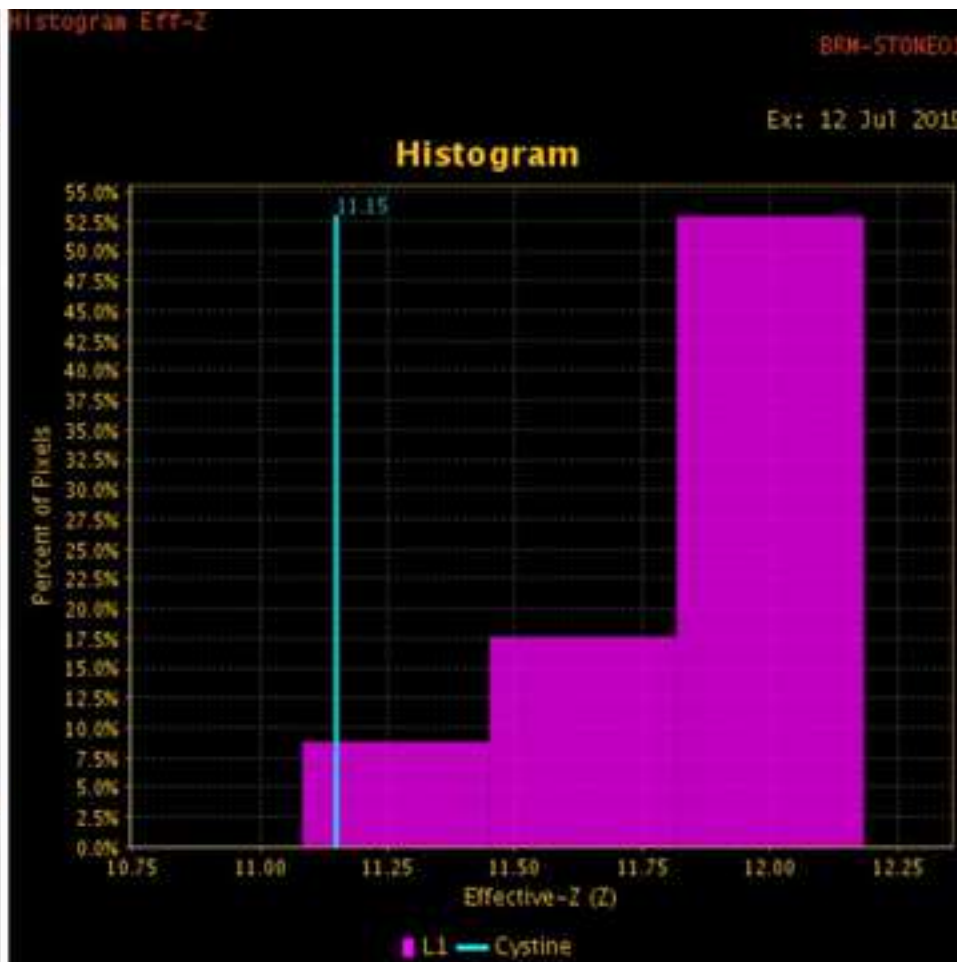


Figure 5

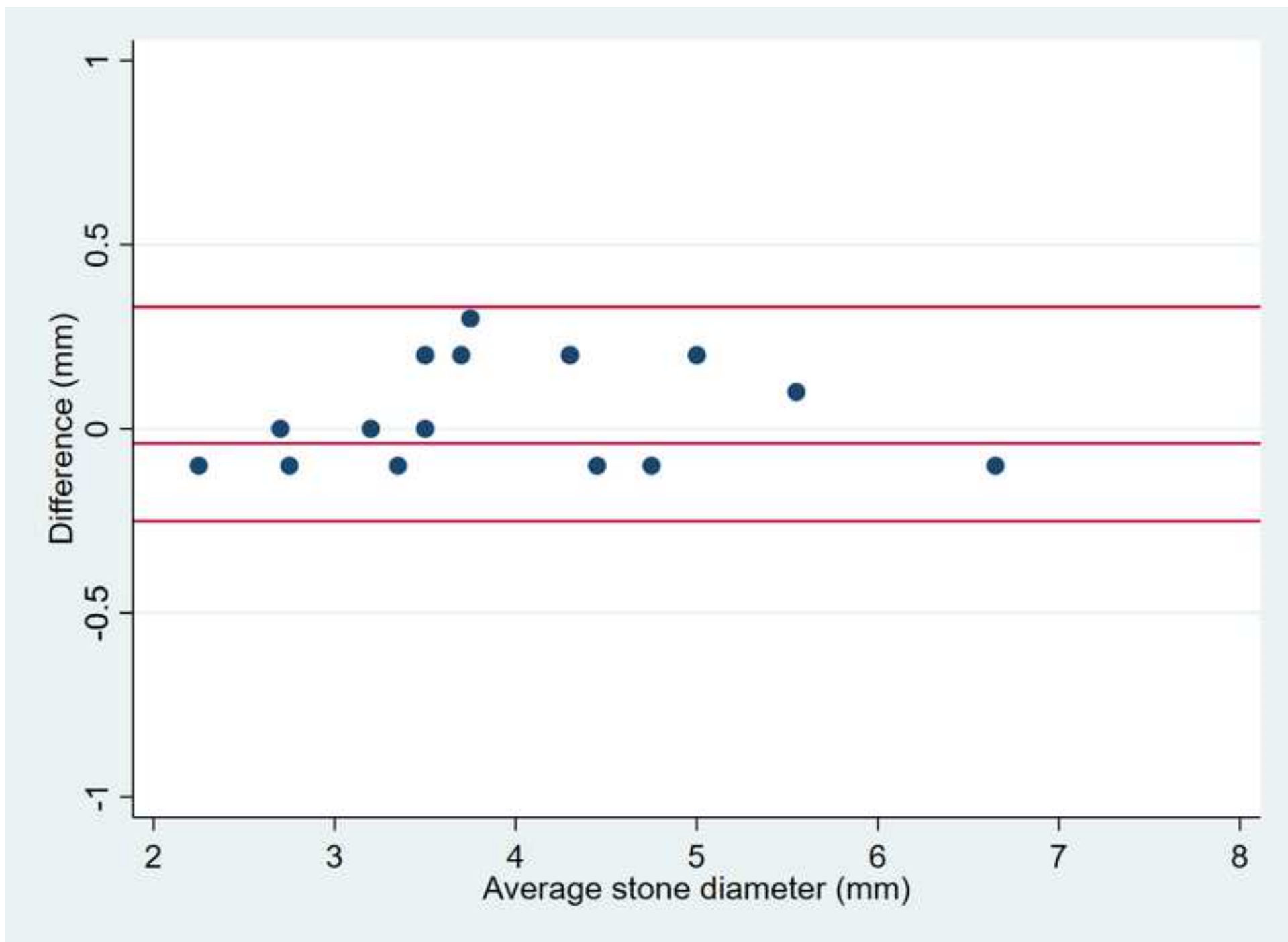


Table 1

	<b>Standard helical</b>	<b>Dual energy</b>
Tube voltage (kV)	120	80/140 fast kV switching
Image Quality Metric	Noise Index 27	Noise Index 27
Reconstruction	40 % ASiR V*	40% ASiR V*
Pitch	0.992	0.992
Rotation time	0.5	0.8
Bowtie filter	Body	Body
Detector configuration	128x0.625	128x0.625
Scan range	195 mm	195 mm
CTDI <sub>vol</sub>	2.60 mGy	7.15 mGy

Table 2

<b>Composition</b>	<b>n</b>	<b>No. correctly identified</b>
Cystine	7	7
Calcium Oxalate	2	1
Uric acid	1	1
Struvite	1	1
Brushite	1	0
Total	12	10

Table 3

	<b>HU<sub>Water</sub></b>	<b>HU<sub>Tissue</sub></b>	<b>SD<sub>Water</sub></b>	<b>SD<sub>Tissue</sub></b>
Standard helical CT	0.9	49.8	25.8	22.0
Dual energy CT	1.6	47.9	23.6	21.0
Difference	0.7	-1.9	-2.2	-1
p-value	0.83	0.40	0.10	0.28

Abbreviations

CaOx	Calcium Oxalate
HU	Hounsfield Units
CT	Computed Tomography
DECT	Dual Energy Computed Tomography
IR	Infrared (spectroscopy)
CTDIvol	Volumetric Computed Tomography Dose Index
MS	Metabolic Syndrome
NIST	National Institute of Science and Technology